S. H. CHANG, S. H. HSIAO

ISSN 0543-5846
METABK 55(1) 33-36 (2016)
UDC – UDK 669.295.24.3:536.42:539.69:621.771:621.785=111

EFFECTS OF TEXTURE ON THE DAMPING CHARACTERISTICS OF COLD-ROLLED AND ANNEALED $Ti_{50}Ni_{40}Cu_{10}$ SHAPE MEMORY ALLOY

Received – Primljeno: 2015-01-29
Accepted – Prihvaćeno: 2015-07-25
Original Scientific Paper – Izvorni znanstveni rad

Cold-rolled and annealed $Ti_{50}Ni_{40}Cu_{10}$ shape memory alloy possesses a major (110)[001] texture along the rolling direction and a minor {111}<uvw> *γ*-fiber texture along the normal direction. The damping capacity of the B2→B19 and B19→B2 martensitic transformation internal friction peaks for the $Ti_{50}Ni_{40}Cu_{10}$ shape memory alloy was more pronounced in the rolling direction than in the transverse direction due to the effects of the cold-rolled and annealed textures. The damping capacity of the B19→B19′ and B19′→B19 martensitic transformation internal friction peaks was not noticeable affected by the orientation of the specimen.

Key words: TiNiCu alloys/shape memory alloys, textures, damping, cold-rolled, annealing

INTRODUCTION

Shape memory alloys (SMAs) are known as functional materials because they present unique properties including the shape memory effect, superelasticity, and high–damping characteristics [1]. Nickel-Titanium (TiNi) SMAs exhibit particular good damping capacity during martensitic transformation; however, they undergo this transformation at temperatures that are not sufficiently high for most applications. It has been reported that substituting Cu for Ni in TiNi SMAs raises the martensitic transformation temperatures and further enhances their damping [2]. The martensitic transformation sequences of $Ti_{50}Ni_{50-x}Cu_x$ SMAs with x < 30 atomic percent (at,%) are complex and closely related to Cu content. In $Ti_{50}Ni_{50-x}Cu_x$ SMAs with a Cu content below 7,5 at,%, the transformation sequence of the alloys is B2↔B19'. When the Cu content of the alloys is between 7,5 at,% and 16 at,%, the transformation sequence of the alloys is a two−stage B2↔B19↔B19'. In $Ti_{50}Ni_{50-x}Cu_x$ SMAs with a Cu content above 16 at,%, the transformation sequence is B2↔B19. Here, B2 is the parent austenite while B19 and B19' are orthorhombic and monoclinic martensites, respectively. The damping properties of $Ti_{50}Ni_{50-x}Cu_x$ SMAs with a variety of martensitic transformation sequences have been widely investigated [3, 4]. Besides, the SME and superelasticity properties found in single crystal SMAs are dependent on its crystal orientation, and the same effects in polycrystalline SMAs are affected by texture [5 - 8]. However, the effects of texture on the damping characteristics of TiNiCu SMAs have yet to be investigated. The main purpose of this study was to investigate the effects of textures produced by cold-rolling on the damping properties of $Ti_{50}Ni_{40}Cu_{10}$ SMA.

EXPERIMENTAL

The $Ti_{50}Ni_{40}Cu_{10}$ SMA in this study was prepared using pure raw titanium, nickel, and copper. The raw materials were re-melted using a vacuum arc furnace to produce a $Ti_{50}Ni_{40}Cu_{10}$ SMA ingot. The as-melted $Ti_{50}Ni_{40}Cu_{10}$ SMA ingot was heated to 900 °C before being hot-rolled to form a plate 2 mm in thickness. Cold-rolling was then applied in the same rolling direction at room temperature, resulting in a plate of 1 mm in thickness (approximately 50 % thickness reduction). Annealing was not performed during cold-rolling to avoid the occurrence of recrystallization. The cold-rolled plate was cut into test specimens using a diamond saw, sealed in an evacuated quartz tube, and annealed at 500 °C for 10 min. Crystallographic features of the cold-rolled and annealed $Ti_{50}Ni_{40}Cu_{10}$ SMA were determined using a Rigaku Ultima IV X-ray diffraction (XRD) instrument with Cu Kα radiation (λ = 0,154 nm). Specimens used in orientation distribution function (ODF) measurements were cut from the annealed plates to the size of 20,0 mm × 15,0 mm × 1,0 mm. ODF specimen was mechanically and electrically polished to a mirror surface. The surface texture of the specimen was calculated from the X-ray pole figure measurements. The pole figures were measured using an X-ray diffractometer with Co-radiation (D8 DISCOVER, Bruker AXS Gmbh, Germany) with Co Kα radiation (λ = 0,179 nm) at room temperature. The ODF, including odd terms and ghost correction, was calculated to an order of l_{max} = 22 using the series expansion method [9]. Damping properties of the cold-rolled and annealed $Ti_{50}Ni_{40}Cu_{10}$ SMA were measured by dy-

S. H. Chang, S. H. Hsiao, National I-Lan University, Taiwan

namic mechanical analysis (DMA). Specimens for the DMA experiments were cut to dimensions of 30,0 mm × 4,0 mm × 1,0 mm, with the long-axis of specimen in the directions of θ = 0° (rolling direction, RD) and 90° (transverse direction, TD) relative to the direction of cold-rolling. The tan δ values of specimen were determined using a TA 2 980 DMA equipped with a single cantilever clamp and liquid nitrogen cooling apparatus. The experiment parameters used in the DMA tests were as follows: cooling rate = 3 °C/min, frequency =1 Hz, and strain amplitude = 8,5 × 10^{-5}.

RESULTS AND DISCUSSION

Figure 1 presents XRD results of the cold-rolled and annealed $Ti_{50}Ni_{40}Cu_{10}$ SMA measured at room temperature. Figure 1 shows a major (110) and a minor (211) diffraction peaks at approximately 2θ = 42° and 77,5°, respectively. The (200) diffraction peak typically found in Ti-Ni-Cu SMAs was not observed in this study. In addition, there is no any pronounced B19 or B19' martensite diffraction peaks can be observed in Figure 1,

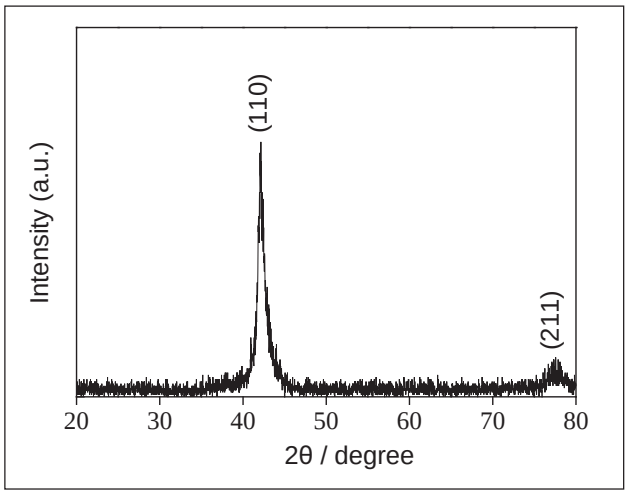

Figure 1 XRD spectra of $Ti_{50}Ni_{40}Cu_{10}$ SMA measured at room temperature

indicating that the cold-rolled and annealed $Ti_{50}Ni_{40}Cu_{10}$ SMA is entirely B2 parent phase at room temperature. Figure 2(a) presents the measured (110) pole figure for the cold-rolled and annealed $Ti_{50}Ni_{40}Cu_{10}$ SMA. The center of the (110) pole figure corresponds to the normal direction (ND) of the specimen surface. Figure 2(a) shows two peaks in the (110) pole figure, symmetrically located in the TD direction. Figure 2(b) shows the calculated (110) pole figure, which is very close to that of the measured one. The measured and calculated of (200) and (210) pole figures were also very similar to each other; however, these figures are not presented in this study. These results indicate that subsequent ODF results calculated from (110), (200) and (210) pole figures will be reliable.

Figure 3(a) presents the three-dimensional ODF results of the cold-rolled and annealed $Ti_{50}Ni_{40}Cu_{10}$ SMA, calculated from the (200), (110) and (210) pole figures. Figure 3(b) shows the φ_2 = 45° section of the contour ODF results in Fig. 3(a), in which most of the preferred orientations are conveniently observed in this section. Figure 3(b) shows that the cold-rolled and annealed $Ti_{50}Ni_{40}Cu_{10}$ SMA possesses a γ-fiber texture in a line at Φ = 55°, resembling {111}<uvw> γ-fiber texture along the ND [5]. This γ-fiber texture along the ND is corresponding to the shearing effect caused by the friction of rollers during cold-rolling process [8]. Figure 3(b) also shows a concentrated (110)[001] texture along the RD, with higher intensity than that of the γ-fiber texture, indicating that the (110)[001] texture is the primary texture in the cold-rolled and annealed $Ti_{50}Ni_{40}Cu_{10}$ SMA.

Figures 4(a) and 4(b) respectively show the DMA tan δ and storage modulus (E-modulus) curves as a function of temperature along the RD and TD in specimens cut from the same cold-rolled and annealed $Ti_{50}Ni_{40}Cu_{10}$ SMA plate. Figure 4(a) shows that the specimen cut along the RD exhibited a pronounced B2→B19 martensitic transformation internal friction peak (tan δ = 0,123) at approximately 33 °C as well as a broad

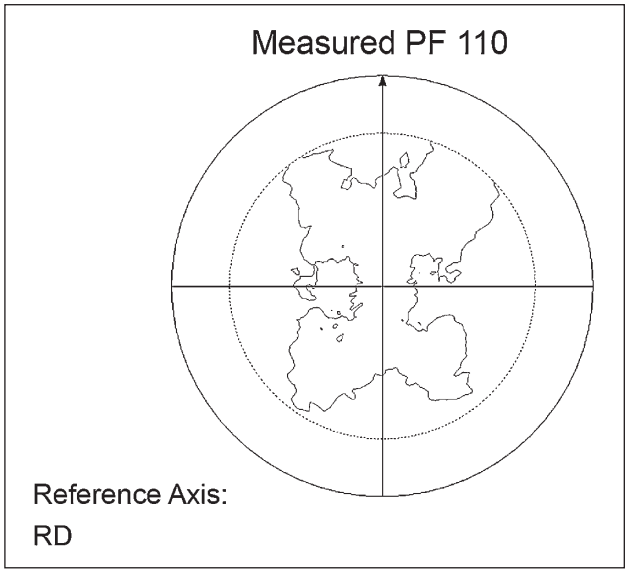

Figure 2a The measured (110) pole figure of $Ti_{50}Ni_{40}Cu_{10}$ SMA

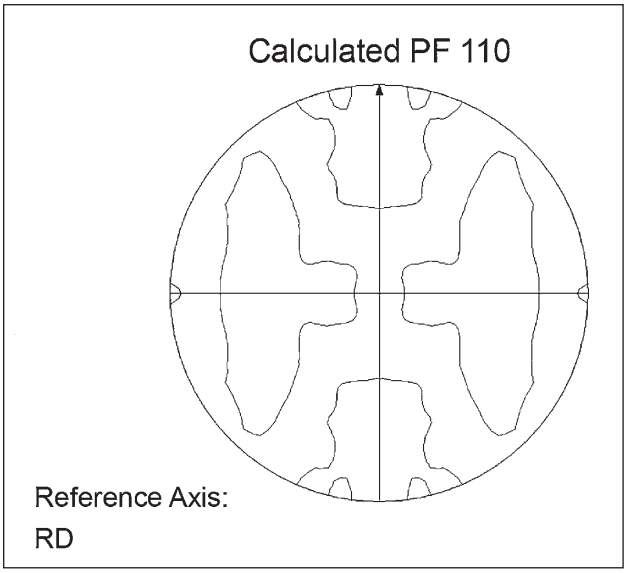

Figure 2b The calculated (110) pole figure of $Ti_{50}Ni_{40}Cu_{10}$ SMA

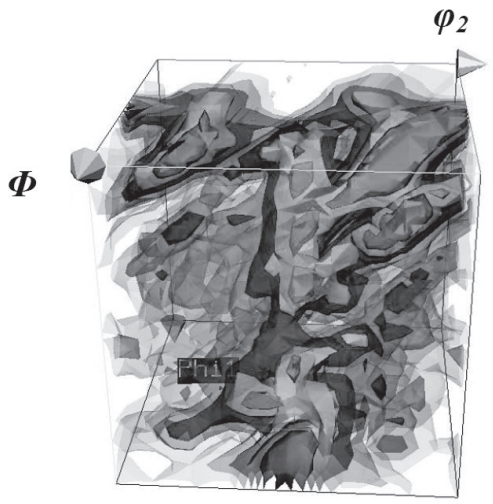

Figure 3a Three-dimensional ODF results of $Ti_{50}Ni_{40}Cu_{10}$ SMA

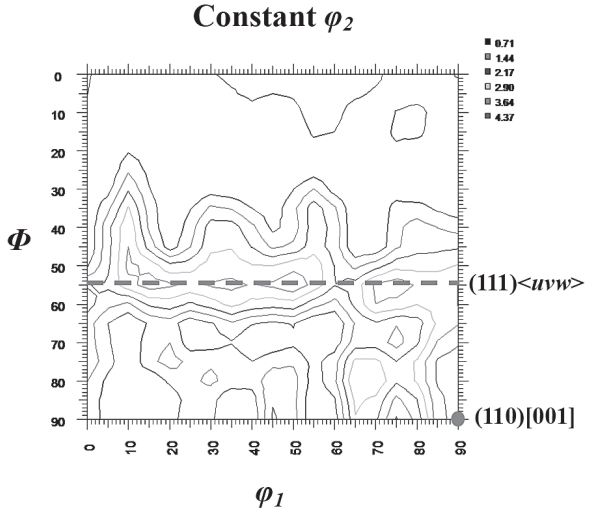

Figure 3b The φ2 = 45° section of the contour ODF results

B19→B19' peak (tan δ = 0,040) at approximately -18 °C in the cooling tan δ curve. The specimen cut along the RD also showed a B19'→B19 peak (tan δ = 0,050) at approximately 38 °C and a significant B19→B2 peak (tan δ = 0,168) at approximately 71 °C in the heating tan δ curve. Figure 4(a) also reveals that the cooling storage modulus curve decreases gently in the B2 parent phase and then reaches a minimum value of approximately 25 500 MPa during B2→B19 martensitic transformation. After B2→B19 martensitic transformation is completed, the storage modulus curve increases with decreasing temperature. The storage modulus curve also shows a minimum value of approximately 25 700 MPa during B19→B2 martensitic transformation in heating. Figure 4(b) shows that the specimens cut along the TD also exhibited B2→B19 and B19→B19' martensitic transformation internal friction peaks in the cooling tan δ curve and B19'→B19 and B19→B2 peaks in heating. However, the tan δ values of the B2→B19 and B19→B2 peaks in the TD sample are only 0,085 and 0,103, respectively. Figure 4(b) also reveals that both the cooling and heating storage modulus curves show a minimum value of approximately 26 500 MPa during the B2→B19 and B19→B 2 martensitic transformations.

According to the ODF results shown in Fig. 3, the cold-rolled and annealed $Ti_{50}Ni_{40}Cu_{10}$ SMA possesses a dominant (110)[001] texture. Previous studies have reported that the (110)[001] texture, which is also observed in other B2 intermetallic compounds such as NiAl, CoTi, and TiNiFe [10, 11], exhibits a possible slip plane system of $(001)[100]_M$ [5]. The Schmid factor of $(001)[100]_M$ is much lower in the TD [5], which results in lower internal friction peaks during the B2→B19 martensitic transformation. According to the DMA results shown in Figs. 4(a) and 4(b), the tan δ values of the B2→B19 and B19→B2 martensitic transformation internal friction peaks for the specimen cut along the RD are higher than those the specimen cut along the TD. This feature indicates that the internal friction of the B2→B19 and B19→B2 martensitic transformation internal friction peaks exhibits anisotropic damping properties due to the effect of the cold-rolled and annealed textures. On the other hand, the tan δ values of the B19→B19' martensitic transformation internal friction peak did not vary between specimens cut along the RD and that cut along the TD (approximately 0,04). These results indicate that the tan δ values of the B19→B19' martensitic transformation internal friction peak are not noticeably affected by the

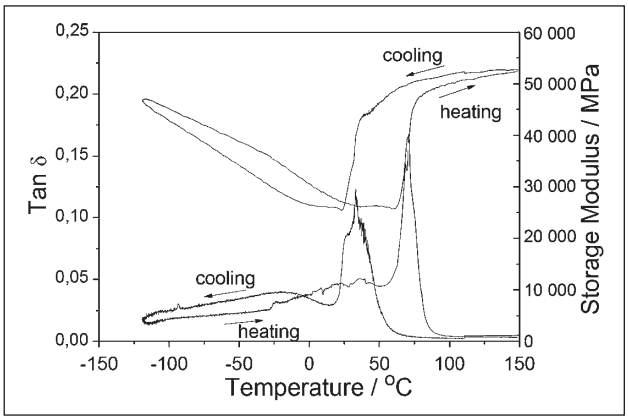

Figure 4a Tan δ and storage modulus curves of $Ti_{50}Ni_{40}Cu_{10}$ SMA in θ = 0° (RD)

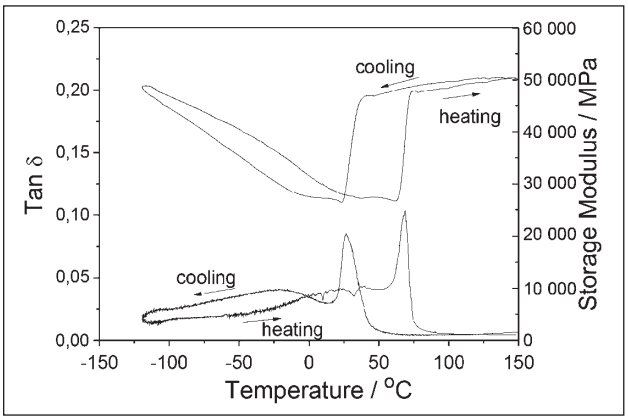

Figure 4b Tan δ and storage modulus curves of $Ti_{50}Ni_{40}Cu_{10}$ SMA in θ = 90° (TD)

orientation of the specimen. This may be due to the fact that the transformation strain involved in B2→B19 martensitic transformation (approximately 8%) is much higher than that of the B19→B19' martensitic transformation (approximately 2%) [1]. However, further investigation will be needed to confirm this.

CONCLUSIONS

Cold-rolled and annealed $Ti_{50}Ni_{40}Cu_{10}$ SMA shows a major (110)[001] texture along the RD and a minor {111}<uvw> γ-fiber texture along the ND. The damping capacity of B2→B19 and B19→B2 martensitic transformation internal friction peaks exhibited anisotropic damping properties resulting from the effects of textures. The damping characteristics of the B19→B19' and B19'→B19 martensitic transformation internal friction peaks did not show significant relation with the textures. The anisotropic damping characteristic is corresponding to the effect of the texture produced during the cold-rolling and annealing process.

Acknowledgement

The authors gratefully acknowledge the financial support for this research provided by the Ministry of Science and Technology (MOST), Taiwan, Republic of China, under Grant No. MOST103-2221-E-197-007.

REFERENCES

[1] K. Otsuka, X. Ren. Physical metallurgy of Ti–Ni-based shape memory alloys. Progress in Materials Science 50 (2005) 511–678.

[2] L. Gou, Y. Liu, T. Y. Ng. An investigation on the crystal structures of Ti50Ni50−xCux shape memory alloys based on density functional theory calculations. Intermetallics 53 (2014) 20-25.

[3] F. M. Mazzolai, A. Biscarini, R. Campanella, B. Coluzzi, G. Mazzolai, A. Rotini, A. Tuissi. Internal friction spectra of the Ni40Ti50Cu10 shape memory alloy charged with hydrogen. Acta Materialia 51 (2003) 573-583.

[4] S. H. Chang, S. H. Hsiao. Inherent internal friction of Ti-50Ni50-xCux shape memory alloys measured under isothermal conditions. Journal of Alloys and Compounds 486 (2014) 69-73.

[5] J. H. Mulder, P. E. Thoma, J. Beyer. Anisotropy of the shape memory effect in tension of cold-rolled 50.8Ti49.2Ni (at. %) sheet, Zeitschrift fur Metallkunde 84 (1993) 501-508.

[6] P. Zheng, N. J. Kucza, Z. Wang, P. Müllnerb, D.C. Dunand. Effect of directional solidification on texture and magnetic-field-induced strain in Ni–Mn–Ga foams with coarse grains. Acta Materialia 86 (2015) 95-101.

[7] R. Dasgupta, A. K. Jain, P. Kumar, S. Hussain, A. Pandey. Role of alloying additions on the properties of Cu–Al–Mn shape memory alloys. Journal of Alloys and Compounds 620 (2015) 60-66.

[8] S. H. Chang, S. K. Wu. Textures in cold-rolled and annealed Ti50Ni50 shape memory alloy. Scripta Materialia 50 (2004) 937-941.

[9] H. J. Bunge. Texture Analysis in Materials Science, London, Butterworths, 1982, pp. 25-29.

[10] M. H. Yoo, T. Takasugi, S. Hanada, O. Izumi. Slip modes in B2-type intermetallic alloys. Materials Transactions JIM 31 (1990) 435-442.

[11] W. J. Moberly, J. L. Proft, T. W. Duerig, R. Sinclair. Deformation, twinning and thermo-mechanical strengthening of Ti50Ni47Fe3. Acta Metallurgica 38 (1990) 2601-2612.

Note: The responsible for English language is Michael D. Ash, Chief Editor of Acceptediting, Taiwan